Oleic and Docosahexaenoic Acid Differentially Phase Separate from Lipid Raft Molecules: A Comparative NMR, DSC, AFM, and Detergent Extraction Study

Saame Raza Shaikh,*† Alfred C. Dumaual,* Alicia Castillo,‡ Daniel LoCascio,* Rafat A. Siddiqui,‡ William Stillwell,*† and Stephen R. Wassall¶†

*Department of Biology, Indiana University-Purdue University, Indianapolis, Indiana; †Medical Biophysics Program, Indiana University School of Medicine, Indianapolis, Indiana; ‡Cellular Biochemistry Laboratory, Methodist Research Institute at Clarian Health, Indianapolis, Indiana; and ¶Department of Physics, Indiana University-Purdue University, Indianapolis, Indiana

ABSTRACT We have previously suggested that the ω-3 polyunsaturated fatty acid, docosahexaenoic acid (DHA) may in part function by enhancing membrane lipid phase separation into lipid rafts. Here we further tested for differences in the molecular interactions of an oleic (OA) versus DHA-containing phospholipid with sphingomyelin (SM) and cholesterol (CHOL) utilizing ^{2}H NMR spectroscopy, differential scanning calorimetry, atomic force microscopy, and detergent extractions in model bilayer membranes. ^{2}H NMR and DSC (differential scanning calorimetry) established the phase behavior of the OA-containing 1-[$^2H_{31}$]palmitoyl-2-oleoyl-*sn*-glycero-3-phosphoethanolamine (16:0-18:1PE-d_{31})/SM (1:1) and the DHA-containing 1-[$^2H_{31}$]-palmitoyl-2-docosahexaenoyl-*sn*-glycero-3-phosphoethanolamine (16:0-22:6PE-d_{31})/SM (1:1) in the absence and presence of equimolar CHOL. CHOL was observed to affect the OA-containing phosphatidylethanolamine (PE) more than the DHA-containing PE, as exemplified by $>2\times$ greater increase in order measured for the perdeuterated palmitic chain in 16:0-18:1PE-d_{31}/SM (1:1) compared to 16:0-22:6PE-d_{31}/SM (1:1) bilayers in the liquid crystalline phase. Atomic force microscopy (AFM) experiments showed less lateral phase separation between 16:0-18:1PE-rich and SM/CHOL-rich raft domains in 16:0-18:1PE/SM/CHOL (1:1:1) bilayers than was observed when 16:0-22:6PE replaced 16:0-18:1PE. Differences in the molecular interaction of 16:0-18:1PE and 16:0-22:6PE with SM/CHOL were also found using biochemical detergent extractions. In the presence of equimolar SM/CHOL, 16:0-18:1PE showed decreased solubilization in comparison to 16:0-22:6PE, indicating greater phase separation with the DHA-PE. Detergent experiments were also conducted with cardiomyocytes fed radiolabeled OA or DHA. Although both OA and DHA were found to be largely detergent solubilized, the amount of OA that was found to be associated with raft-rich detergent-resistant membranes exceeded DHA by almost a factor of 2. We conclude that the OA-PE phase separates from rafts far less than DHA-PE, which may have implications for cellular signaling.

INTRODUCTION

It is well recognized that dietary intake of ω-3 polyunsaturated fatty acids (PUFAs) has profound benefits on normal health and prevention of chronic disease states, although the molecular mechanism responsible remains unclear. One possibility is that ω-3 PUFAs are incorporated into the plasma membrane, influencing membrane structure and function (Jump, 2002; Stillwell, 2000). Of special importance for human health is docosahexaenoic acid (DHA), the longest and most unsaturated fatty acid commonly found in the plasma membrane. With 22 carbons and 6 *cis* double bonds located at positions 4, 7, 10, 13, 16, and 19, DHA's unique molecular structure (Eldho et al., 2003) renders it a primary candidate for affecting properties of the membrane. It has been proposed by us (Brzustowicz et al., 2002a; Shaikh et al., 2002) and others (Huster et al., 1998; Mitchell and Litman, 1998) that DHA may be specifically involved in inducing lateral phase separations into DHA-rich/cholesterol-poor and DHA-poor/cholesterol-rich lipid microdomains. A reduced affinity between the DHA acyl chain and cholesterol has been hypothesized to promote phase separations, perhaps affecting lipid rafts (Stillwell and Wassall, 2003).

Lipid rafts are postulated to be specialized liquid-ordered (l_o) lipid microdomains rich in sphingolipids and cholesterol. They are involved in serving as platforms for cellular signaling events (Ahmed et al., 1997; Edidin, 1993, 2003a; Hooper, 1999) by accumulating specific proteins, including GPI-anchored proteins and the src-family of kinases. In addition, rafts are thought to influence lipid trafficking events, pathogen entry, and cytoskeletal organization (Munro, 2003). The supposed stability of lipid rafts is attributed to the favorable interaction between the amide of the sphingosine backbone and the hydroxyl of an adjacent sphingolipid as well as hydrogen bonding between the 3-OH of cholesterol and the sphingosine amide. Saturated acyl chains are thought to promote formation of rafts since they are more extended than unsaturated chains and pack well amongst themselves and with cholesterol. Consequently, phospholipids containing highly disordered polyunsaturated

Submitted April 16, 2004, and accepted for publication June 18, 2004.

Address reprint requests to William Stillwell, Dept. of Biology, Indiana University-Purdue University, 723 W. Michigan St., Indianapolis, IN 46202-5132. Tel.: 317-274-0580; Fax: 317-274-2846; E-mail: wstillwe@iupui.edu.

0006-3495/04/09/1752/15 $2.00

doi: 10.1529/biophysj.104.044552

acyl chains that exhibit low affinity to cholesterol would be expected to phase separate from the rafts.

We suggested in a preliminary investigation that an oleic acid (OA)-containing phosphatidylethanolamine (PE) and a DHA-containing PE may phase separate differently from the lipid raft molecules sphingomyelin (SM) and cholesterol (CHOL) in monolayer and bilayer membranes (Shaikh et al., 2002). Here we elucidate the effect that replacing the OA-containing 1-palmitoyl-2-oleoyl-*sn*-glycero-3-phosphoethanolamine (16:0-18:1PE) with the DHA-containing 1-palmitoyl-2-docosahexaenoyl-*sn*-glycero-3-phosphoethanolamine (16:0-22:6PE) has on phase separation from SM and CHOL. PE was chosen as our model phospholipid since it is the second most abundant polar lipid found in mammalian plasma membranes and it is often in PE that DHA accumulates (Simopoulos et al., 1986; Zerouga et al., 1996). Partial lipid asymmetry is a characteristic of all membranes. Approximately one-sixth of plasma membrane PE is found in the outer leaflet where it would interact with the abundant SM (approximately five-sixths of the total SM). In the inner leaflet, the abundant PE (approximately five-sixths of the total PE) would interact with the less abundant SM (approximately one-sixth of the total SM). Therefore, in both membrane leaflets there are sufficient quantities of both PE and SM to affect membrane structure (Simons and Vaz, 2004). PEs normally exist as heteroacid *sn*-1 saturated, *sn*-2 unsaturated species. We employ 16:0-18:1PE as our ''typical'' phospholipid because oleic acid is the most abundant unsaturated fatty acid in membranes and 16:0-22:6PE constitutes our ''modified'' phospholipid.

In this study we explore differences in lateral phase separation between 16:0-18:1PE/SM/CHOL (1:1:1) and 16:0-22:6PE/SM/CHOL (1:1:1) bilayers employing solid state ^{2}H NMR spectroscopy, differential scanning calorimetry (DSC), atomic force microscopy (AFM), and detergent extraction. ^{2}H NMR and DSC are first used to characterize the phase behavior of our model membrane systems in the absence and presence of cholesterol. Subsequent analysis of ^{2}H NMR spectra in the lamellar liquid crystalline phase, AFM measurements, and detergent-resistant experiments in model membranes demonstrate marked differences in the molecular interactions of 16:0-18:1PE versus 16:0-22:6PE with raft molecules. We also extend our studies to include detergent-resistant studies with living cardiomyocytes. These studies are discussed in relation to the physiological importance of rafts.

MATERIALS AND METHODS

Materials

Egg SM, 1-palmitoyl-2-oleoyl-*sn*-glycero-3-phosphoethanolamine (16:0-18:1PE), 1-[$^2H_{31}$]palmitoyl-2-oleoyl-*sn*-glycero-3-phosphoethanolamine (16:0-18:1PE-d_{31}), 1-palmitoyl-2-docosahexaenoyl-*sn*-glycero-3-phosphoethanolamine (16:0-22:6PE), and 1-[$^2H_{31}$]palmitoyl-2-docosahexaenoyl-*sn*-glycero-3-phosphoethanolamine (16:0-22:6PE-d_{31}) were purchased from Avanti Polar Lipids (Alabaster, AL). CHOL was obtained from Sigma Chemical Co. (St. Louis, MO). Lipid purity was assessed with thin layer chromatography. Lipid and cholesterol concentrations were quantified using phosphate and gravimetric analyses, respectively. Deuterium-depleted H_2O used in the ^{2}H NMR studies was obtained from Isotec (Miamisburg, OH). High-performance thin layer chromatography (HPTLC) plates were purchased from Alltech (Deerfield, IL). All organic solvents were HPLC grade and obtained from Fisher Scientific (Pittsburgh, PA). Molecular Probes (Eugene, OR) was the source of cholera toxin subunit B, horseradish peroxidase conjugate. The radiolabeled fatty acids [^{14}C]DHA and [^{3}H]OA were obtained from PerkinElmer (Boston, MA) The cardiomyocyte isolation kit was purchased from Worthington Biochemical (Lakewood, NJ). Horse and fetal bovine serums were from Hyclone (Logan, UT).

^{2}H NMR sample preparation

^{2}H NMR samples were prepared taking stringent precautions to prevent oxidation, as described before (Shaikh et al., 2002). Lipid mixtures containing 100 mg total lipid were codissolved in chloroform, dried under argon gas, and placed under vacuum overnight. After vacuum pumping, the mixtures were hydrated to 50 wt % with 50 mM Tris buffer (pH 7.4) and vigorously vortexed for ~5 min. The pH was corrected in the presence of 2 mL additional deuterium-depleted H_2O, and the samples were then frozen and lyophilized multiple times at ~50 mTorr to reduce the ^{2}H NMR signal from residual ^{2}HHO. After hydrating the powders to 50 wt %, the resultant aqueous multilamellar dispersions were transferred to 5-mm glass NMR tubes and stored at −20°C when not in use. All samples were allowed to equilibrate to room temperature for ~1 h before experimentation. As previously reported (Brzustowicz et al., 2002b; Shaikh et al., 2002), we have compared phospholipid/cholesterol samples prepared as described here and by the low-temperature trapping method (Huang et al., 1999) designed to ensure that lipids do not demix during removal of the solvent. Both methods yielded essentially identical results.

^{2}H NMR spectroscopy

Solid-state ^{2}H NMR spectra were acquired on a home-built spectrometer operating at a resonance frequency of 27.6 MHz. A double resonance probe (Cryomagnet Systems, Indianapolis, IN) with a 5-mm transverse-mounted coil was utilized. Temperature was controlled (±0.5°C) with a Love Controls (1600 series) temperature controller (Michigan City, IN). Spectral parameters were as stated previously (McCabe et al., 1994; Shaikh et al., 2003a).

Analysis of ^{2}H NMR spectra

Moments M_n were calculated from ^{2}H NMR spectra for 16:0-18:1PE-d_{31} or 16:0-22:6PE-d_{31} in PE/SM (1:1) and PE/SM/CHOL (1:1:1) mixtures with

$$M_n = \frac{\int_{-\infty}^{\infty} |\omega^n| f(\omega) d\omega}{\int_{-\infty}^{\infty} f(\omega) d\omega}, \quad (1)$$

where ω is the frequency with respect to the central Larmor frequency ω_0, $f(\omega)$ is the lineshape, and n is the order of the spectral moment (Davis, 1983). In practice the integral is a summation over the digitized data. The expression

$$M_1 = \frac{\pi}{\sqrt{3}} \left(\frac{e^2 qQ}{h} \right) |\overline{S}_{CD}| \quad (2)$$

relates the first moment M_1 to the average order parameter $\overline{S}_{CD}$ of the perdeuterated palmitic *sn*-1 chain *via* the static quadrupolar coupling constant $(e^2qQ/h) = 167$ kHz in the lamellar liquid crystalline phase.

Spectra were also fast Fourier transform (FFT) depaked to enhance resolution in the lamellar liquid crystalline phase (McCabe and Wassall, 1997). The depaking procedure numerically deconvolutes the powder pattern signal to a spectrum representative of a planar membrane of single alignment. The depaked spectra consist of doublets with quadrupolar splittings $\Delta\nu(\vartheta)$ that equate to order parameters by

$$\Delta\nu(\theta) = \frac{3}{2}\left(\frac{e^2qQ}{h}\right)|S_{CD}|P_2(\cos\theta), \quad (3)$$

where $\vartheta = 0°$ is the angle the membrane normal makes with the magnetic field and $P_2(\cos\vartheta)$ is the second-order Legendre polynomial. Smoothed profiles of order along the perdeuterated palmitoyl *sn*-1 chain were then constructed on the basis of integrated intensity assuming monotonic variation toward the disordered center of the bilayer (Lafleur et al., 1989).

Differential scanning calorimetry

DSC experiments were conducted as previously described (Shaikh et al., 2001). Briefly, lipid mixtures, codissolved in chloroform, were dried under argon gas followed by ~12 h under vacuum to ensure the removal of residual organic solvent. Samples containing DHA were prepared under dark conditions in a glovebox with an argon atmosphere to control for oxidation. Multilamellar vesicles (MLVs) were made by hydrating the appropriate phospholipids at 5 mg/ml in 10 mM sodium phosphate buffer (pH 7.4) with subsequent removal of oxygen. MLV solutions were frozen in dry ice and thawed three times in a water bath above the gel-to-liquid crystalline phase transition temperature (T_m) of the lipids. The MLV solutions (500 μL) were added to each of the three chambers of a Calorimetry Sciences differential scanning calorimeter (American Fork, Utah) whereas the fourth chamber contained 500 μL of the buffer. Heating and cooling scans were made at 0.125°C/min. Only the cooling scans are presented although data derived from both scans appeared nearly identical. Deconvolution of the multicomponent 16:0-18:1PE/SM (1:1) scan was accomplished with Microcal Origin Software (Northampton, MA).

AFM sample preparation

Lipid mixtures codissolved in chloroform were dried under argon gas and placed in a vacuum overnight. Two mL of buffer solution (10 mM MOPS, 200 mM NaCl, 0.1 μM EGTA, pH 7.4) warmed above the phase transition was added to the dried lipid film at a final concentration of 1 mM to make MLVs as described above. Large unilamellar vesicles (LUVs) of 0.1 μm diameter were formed by initially extruding the MLV suspension multiple times through a 1.0-μm pore-sized nucleopore polycarbonate filter (Whatman, Clifton, NJ) and subsequently through a 0.1-μm nucleopore filter using a miniextruder (Avanti Polar Lipids). Fifty-nm diameter small unilamellar vesicle (SUV) lipid suspensions were made by additionally passing the LUV suspension through a 0.05-μm nucleopore filter. Lipid preparation and AFM experiments were conducted in the dark and under degassed, argon gas-saturated conditions to prevent oxidation.

Supported bilayers

Supported bilayer formation using LUV suspensions was adapted from Tokumasu et al (2003). Briefly, 20 μL of the LUV suspension was placed on a freshly cleaved mica surface, incubated for 30–60 s, and then washed with buffer. Excess solution was removed and fresh degassed buffer solution was added to the sample and allowed to incubate for 30–60 min before imaging. Alternatively, supported bilayers were also formed using an SUV suspension (Rinia et al., 2002). In this case, 75 μL of the SUV suspension with a lipid concentration of ~0.5 mM was added to the freshly cleaved mica surface. Lipid vesicles were allowed to absorb to the mica surface for a period of 10 h at 4°C. Afterwards, the sample was rinsed with buffer solution and warmed above the phase transition temperature for 60 min and then allowed to cool to room temperature. Samples were rinsed once more and fresh, degassed buffer solution was added before imaging. Images from LUV and SUV vesicle deposition showed nearly identical results.

Atomic force microscopy

Supported bilayer samples were placed in a liquid cell holder attached to a Bioscope AFM (Digital Instruments, Santa Barbara, CA) set on a vibration-free air table. Bilayer surfaces were imaged using the tapping mode at a scanning rate of 0.5–1.0 Hz and a tapping frequency of ~7.8 kHz using DNP-S20 oxide-sharpened tips with a spring constant of 0.06 N/m (Digital Instruments). All images were scanned over a 10 × 10-μm area at room temperature (23°C). Images were acquired from four separate experiments for each lipid composition with a minimum of four images (from separate areas of the bilayer) per experiment for analysis. Image analysis was conducted with software provided by Digital Instruments in addition to NIH Image J software.

Detergent-resistant studies

Detergent-resistant studies were conducted as described by others (Gandhavadi et al., 2002; Schroeder et al., 1994). Lipid mixtures (2 mg) of either 16:0-18:1PE/SM/CHOL (1:1:1) or 16:0-22:6PE/SM/CHOL (1:1:1) were codissolved in chloroform and dried under a gentle stream of argon gas. Samples were then placed in a vacuum for a minimum of ~6 h to remove trace amounts of organic solvent. MLVs were prepared by adding 1 mL of phosphate-buffered saline (PBS) (Cambrex, East Rutherford, NJ) into the samples and hydrating them for 30 min at 45°C with intermittent vortexing. MLVs were then incubated at 4 or 40°C for 30 min in the presence of 1% Triton X-100 and subsequently centrifuged at the appropriate temperature in a Beckman (Fullerton, CA) table-top centrifuge (TL100) for 1 h at 200,000 *g*. Supernatants (detergent soluble membranes, DSMs) and pellets (detergent resistant membranes, DRMs) were separated and washed for 90 min with SM-2 Adsorbent Bio-Beads (Bio-Rad, Hercules, CA) to remove Triton X-100 (Gandhavadi et al., 2002). DSMs and DRMs were lyophilized for ~10 h to remove H_20 and then dissolved in chloroform and subjected to HPTLC analysis.

HPTLC analysis

SM, CHOL, and PE lipids were separated as described (Graham and Higgins, 1997) on HPTLC plates. Plates were developed (halfway up the plate) twice in chloroform-methanol-water (60:30:5 by volume) followed by a third development (to the top of the plate) with hexane-diethyl ether-acetic acid (80:20:1.5 by volume). They were then charred (~190°C) in 5% $CuSO_4$/4% H_3PO_4 solution for 10 min and analyzed using a Kodak Image Station.

Isolation of cardiomyocytes and cell culture

Neonatal cardiomyocytes were isolated using a cell isolation system from Worthington Biochemical (Lakewood, NJ). Hearts were isolated from 1- to 3-day-old Wistar rats. Connective tissue and atria were removed from the hearts and ventricles were subsequently minced into ~1-mm blocks and digested with trypsin overnight. Trypsin activity was neutralized the following day and tissues were further digested with collagenase. Single-cell isolation was achieved by filtering the cell suspension through a 70-μm filter. Cells were then preplated to remove fibroblasts and cardiomyocytes were isolated using the isolation protocol accompanying the kit (Worthington). Dead cells and cellular debris were removed by centrifugation on a

5-mL Opti-Prep density gradient solution (Axis-Shiel PoC, As, Oslo, Norway). Isolated neonatal cardiomyocytes were cultured for 24 h in a humidified incubation chamber in the presence of 95% O_2/5% CO_2 on laminin- and collagen-coated plates in F-10 media (containing 10% horse serum, 5% fetal bovine serum, 100 units/mL penicillin, 100 μg/mL streptomyocin, and 0.1 mM bromodeoxyuridine).

Incorporation of radiolabeled fatty acids

Cardiomyocytes were washed with serum-free media twice and then treated with 5 μM DHA or OA in the presence of trace amounts of [^{14}C]DHA (0.2 μCi/mL) and [^{3}H]OA (1 μCi/mL), respectively, under serum-free conditions for 24 h. Free fatty acid solutions containing radiolabeled fatty acids were prepared freshly each time from stock solutions by dissolving the compounds in EtOH with a final EtOH concentration in warmed culture medium $\leq$0.05%. The concentration of free fatty acids used was based on cell viability measurements using WST-1 (Roche Biochemicals, Indianapolis, IN).

Isolation of detergent-resistant membranes

Cells were scraped and dissolved in 1 mL of cold Mes-buffered saline (MBS; 150 mM NaCl, 25 mM Mes, pH 6.5) in the presence of 1% (w/v) Triton X-100. Cells were incubated for 30 min at 4°C and then homogenized on ice. Cold MBS (1.5 mL) was added to the homogenate and 2 mL of this suspension was mixed with 2 mL of 90% (w/v) sucrose in MBS. The mixture was then added onto a sucrose gradient consisting of 8 mL of 5–35% (w/v) sucrose in MBS. All solutions were supplemented with a protease inhibitor cocktail (Roche Biochemicals). Sucrose gradients were then subjected to centrifugation in a Beckman SW40 (Fullerton, CA) swinging bucket rotor at 200,000 *g* for 20 h at 4°C. Fractions of 1 mL each were collected from the top to the bottom of the tubes, vortexed, and stored at −80°C until further use. Fifty μL of each isolated sucrose gradient fraction containing [^{3}H]OA or [^{14}C]DHA was placed in a scintillation vial, mixed with scintillation fluid, and counted using a Beckman scintillation counter (LS 6000 IC).

β-cholera toxin binding to GM1

Dot blots were obtained to test for localization of GM1, a raft marker (Brown and London, 2000), in sucrose gradient fractions of cardiomyocytes. Twenty μL of each fraction was loaded onto a nitrocellulose paper and placed under a vacuum for 2 h. The nitrocellulose was then blocked in Blocker Blotto (Pierce, Rockford, IL) for 1 h and then incubated in peroxidase labeled β-cholera toxin overnight (1:1000) in TTBS (50 mM Tris-HCl, 150 mM NaCl, 0.05% Tween-20, pH 7.4) in the cold. Blots were then washed three times in TTBS buffer and developed using an enhanced-chemiluminescence kit and x-ray film. X-ray films were quantified using a Kodak Image Station.

RESULTS

Characterization of phase behavior for 16:0-18:1PE-d_{31}/SM (1:1) versus 16:0-22:6PE-d_{31}/SM (1:1) in the absence and presence of equimolar CHOL

Fig. 1 presents ^{2}H NMR spectra for aqueous multilamellar dispersions of 16:0-18:1PE-d_{31}/SM (1:1) and 16:0-22:6PE-d_{31}/SM (1:1) at 5, 25, and 40°C. The approach is to use the perdeuterated *sn*-1 chain as an intrinsic probe of molecular organization for the phospholipid in the manner advocated by, for example, Petrache et al. (2001) who examined DHA-containing phosphatidylcholines (PCs) with a series of saturated *sn*-1 chains. Both 16:0-18:1PE-d_{31}/SM (1:1) (Fig. 1 *a*) and 16:0-22:6PE-d_{31}/SM (1:1) (Fig. 1 *d*) at 5°C show featureless broad spectra characteristic of the gel phase with shoulders at $\pm$63 kHz. The spectral shape is rendered nonaxially symmetric (asymmetry parameter $\eta \neq 0$) by slow rotational diffusion of the all *trans* 16:0 acyl chains (Wassall et al., 1986). Increasing the temperature to 25°C results in a narrowing of the spectra to $\pm$19 kHz for 16:0-18:1PE-d_{31}/SM (1:1) (Fig. 1 *b*) and $\pm$16 kHz for 16:0-22:6PE-d_{31}/SM (Fig. 1 *e*), indicating fast axial rotation associated with the onset of lamellar liquid crystalline phase. Spectra recorded at 40°C for 16:0-18:1PE-d_{31}/SM (1:1) (Fig. 1 *c*) and 16:0-22:6PE-d_{31}/SM (1:1) (Fig. 1 *f*) are characterized by spectral edges at $\pm$15 kHz, and are representative of the lamellar liquid crystalline phase in which there is rapid isomerization about the carbon-carbon bonds.

Fig. 2 illustrates the effect of equimolar CHOL on the phase behavior of 16:0-18:1PE-d_{31}/SM (1:1) and 16:0-22:6PE-d_{31}/SM (1:1) bilayers at 5, 25, and 40°C. All samples at 5, 25, and 40°C produce powder patterns characteristic of the liquid crystalline state. Although spectral peaks at 5°C are poorly resolved for 16:0-18:1PE-d_{31}/SM/CHOL (1:1:1) (Fig. 2 *a*) and 16:0-22:6PE-d_{31}/SM/CHOL (1:1:1) (Fig. 2 *d*), particularly in the former system, the PE component in either lipid mixture displays spectral edges at $\pm$28 kHz, indicative of fast axial rotation. Upon increasing the temperature to 25 or 40°C enhanced spectral resolution becomes apparent and a differential reduction in width is observed between 16:0-18:1PE-d_{31}/SM/CHOL (1:1:1) (Fig. 2, *b* and *c*) and 16:0-22:6PE-d_{31}/SM/CHOL (1:1:1) (Fig. 2, *e* and *f*). The sharp edges of the spectrum for 16:0-18:1PE-d_{31}/SM/CHOL (1:1:1) bilayers occur at $\pm$25 kHz (25°C) and $\pm$23 kHz (40°C) in comparison to $\pm$22 kHz (25°C) and $\pm$19 kHz (40°C) for 16:0-22:6PE-d_{31}/SM/CHOL (1:1:1). A greater increase in order due to the sterol for the OA-containing component than the DHA-containing component in the mixtures with SM is indicated.

Figs. 1 and 2 only present examples of spectra at selected temperatures. However, spectra for 16:0-18:1PE-d_{31}/SM (1:1), 16:0-18:1PE-d_{31}/SM/CHOL (1:1:1), 16:0-22:6PE-d_{31}/SM (1:1), and 16:0-22:6PE-d_{31}/SM/CHOL (1:1:1) were acquired over a wide temperature range from −10 to 40°C. To illustrate the effect of temperature on phase behavior, Fig. 3, *a* and *b*, presents the first moment M_1 as a function of temperature for all four of the lipid mixtures. For 16:0-18:1PE-d_{31}/SM (1:1) bilayers (Fig. 3 *a*), adoption of gel phase by 16:0-18:1PE-d_{31} is signified by $M_1 > 10 \times 10^4$ s^{-1} for temperatures <20°C. The liquid crystalline state, characterized by $M_1 < 6.5 \times 10^4$ s^{-1}, was adopted at temperatures >25°C. The sharp drop in M_1 value that accompanies the gel-to-liquid crystalline phase transition is centered at ~23°C (represented by *X* in Fig. 3 *a*). There is no longer a discontinuity in the temperature variation of the first moment after the addition of equimolar CHOL to 16:0-18:1PE-d_{31}/SM (1:1) (Fig. 3 *a*). The values gradually

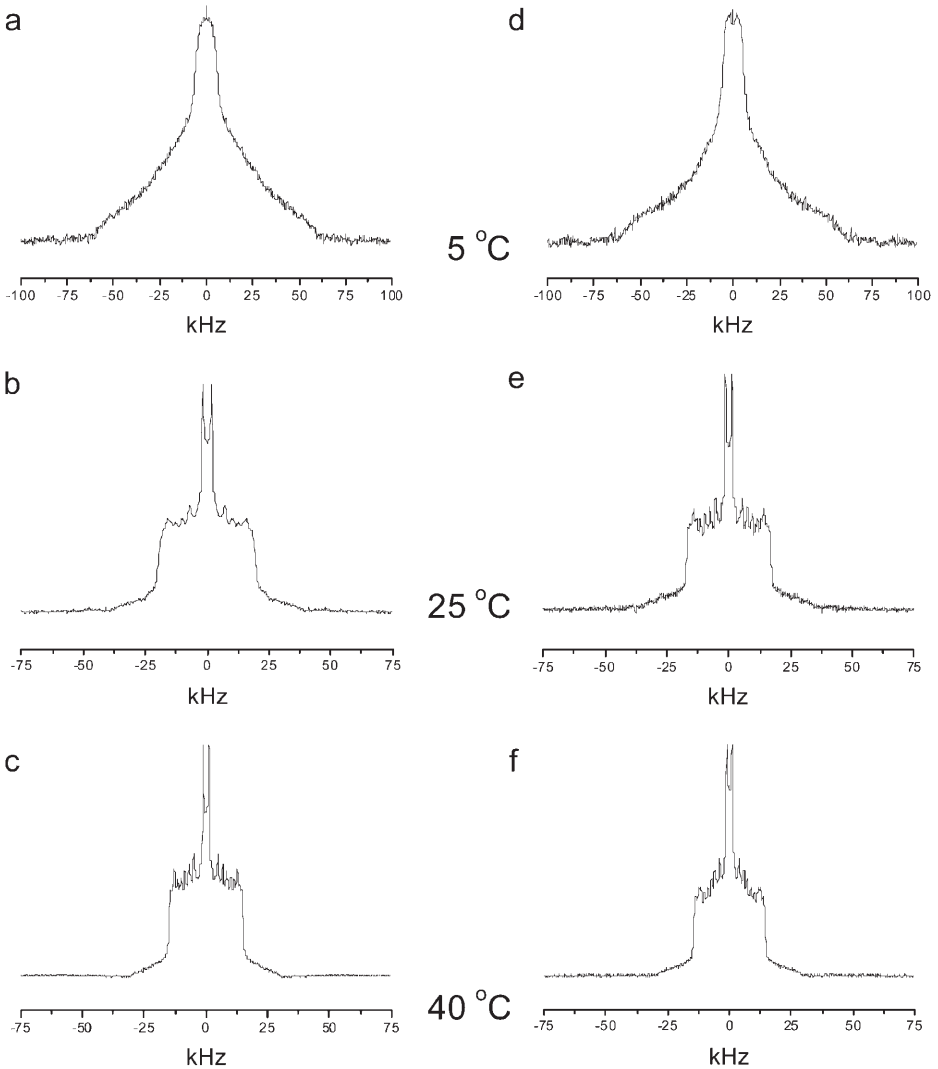

FIGURE 1 ^{2}H NMR spectra for 50 wt % aqueous dispersions in 50 mM Tris buffer (pH 7.4) of 16:0-18:1PE-d_{31}/SM (1:1) and 16:0-22:6PE-d_{31}/SM (1:1). Spectra for 16:0-18:1PE-d_{31}/SM (1:1) were recorded at (*a*) 5, (*b*) 25, and (*c*) 40°C. Spectra for 16:0-22:6PE-d_{31}/SM (1:1) were also recorded at (*d*) 5, (*e*) 25, and (*f*) 40°C.

decrease (10.5–8.0 $\times$ 10^4 s^{-1}) over the temperature range plotted, indicating a broadening of the phase transition to near obliteration.

For 16:0-22:6PE-d_{31}/SM (1:1) (Fig. 3 *b*) bilayers, $M_1 >$ 10 $\times$ 10^4 s^{-1} characterized the lamellar gel phase corresponding to temperatures <5°C. The lamellar liquid crystalline phase exists at temperatures >10°C, where $M_1 <$ 7 $\times$ 10^4 s^{-1}. The abrupt change in M_1 that accompanies the chain melting transition of 16:0-22:6PE-d_{31} in the mixed membrane occurs at ~7°C (represented by *X* in Fig. 3 *b*). The moments for 16:0-22:6PE-d_{31}/SM (1:1) also demonstrate that SM serves to stabilize the bilayer. They signify the lamellar phase throughout the temperature range studied, whereas we detected a transition to the inverted hexagonal phase at T_h = 13°C for 16:0-22:6PE-d_{31} with ^{2}H NMR spectroscopy (Shaikh et al., 2003a). The moments for 16:0-22:6PE-d_{31}/SM/CHOL (1:1:1) continuously decrease (10.5–5.7 $\times$ 10^4 s^{-1}) from −10 to 40°C (Fig. 3 *b*). As with 16:0-18:1PE-d_{31}/SM/CHOL (1:1:1), a lack of sharp discontinuity in the M_1 values indicates that the chain-melting transition for the labeled PE component within the mixed membrane has been broadened beyond detection by the introduction of sterol. On the basis of spectral moments measured for 16:0-22:6PE-d_{31}, we previously found that a gel-to-liquid crystalline transition remained when equimolar cholesterol was added to the polyunsaturated membrane (Shaikh et al., 2003a). The implication is that both sphingomyelin and sterol contribute to the broadening of the transition for 16:0-22:6PE-d_{31} in 16:0-22:6PE-d_{31}/SM/CHOL (1:1:1).

Fig. 3 also presents DSC cooling scans, for comparative purposes, for 16:0-18:1PE/SM (1:1) (Fig. 3 *c*) and 16:0-22:6PE/SM (1:1) (Fig. 3 *d*) bilayers in the absence and presence of equimolar CHOL. The cooling scan for 16:0-18:1PE/SM (1:1) (Fig. 3 *c*) displays a broad exotherm, which was deconvoluted into two transitions (Fig. 3, *inset*) that we ascribe to 16:0-18:1PE-rich/SM-poor (T_m = 26.1°C) and 16:0-18:1PE-poor/SM-rich (T_m = 30.1°C) transitions. The clear observation of two separate exotherms at other PE/SM ratios provided a rationale for deconvolution with the 1:1

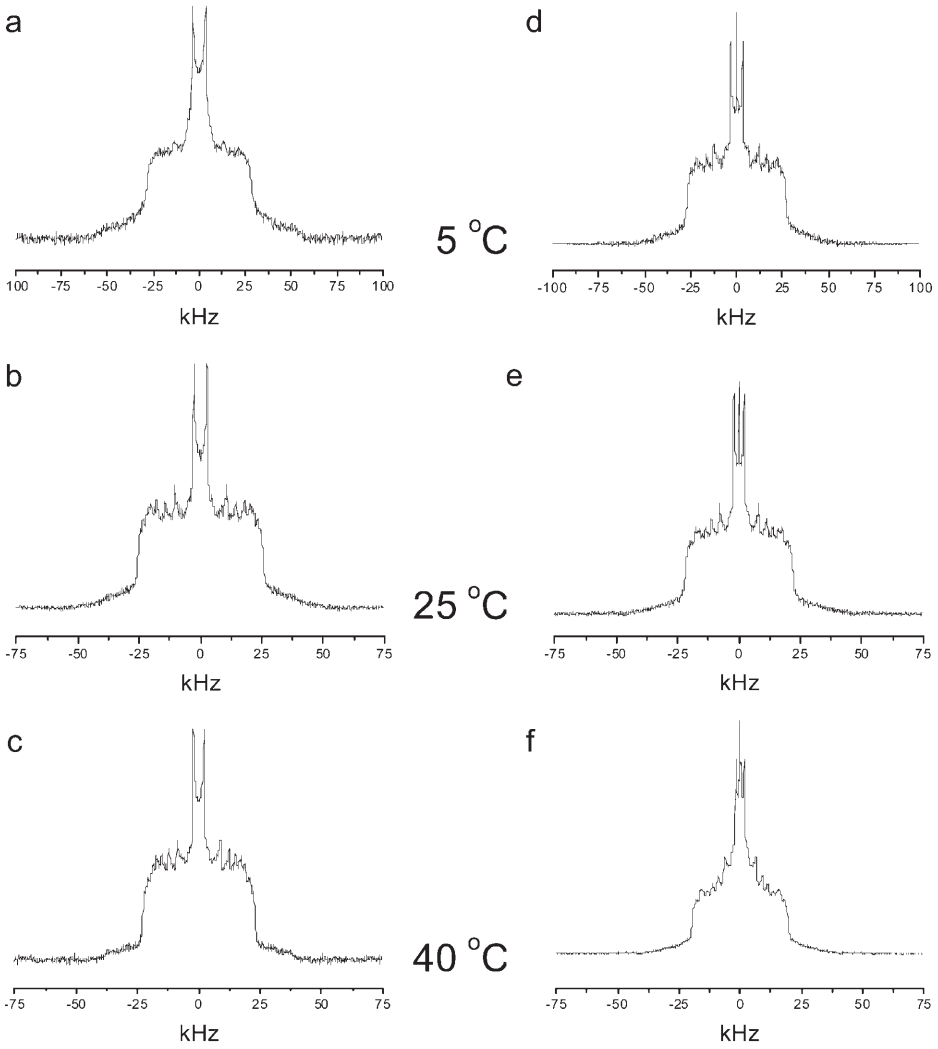

FIGURE 2 ^{2}H NMR spectra for 50 wt % aqueous dispersions in 50 mM Tris buffer (pH 7.4) of 16:0-18:1PE-d_{31}/SM/CHOL (1:1:1) and 16:0-22:6PE-d_{31}/SM/CHOL (1:1:1). Spectra for 16:0-18:1PE-d_{31}/SM/CHOL (1:1:1) were recorded at (*a*) 5, (*b*) 25, and (*c*) 40°C. Spectra for 16:0-22:6PE-d_{31}/SM/CHOL were also recorded at (*d*) 5, (*e*) 25, and (*f*) 40°C.

mixture (Shaikh et al., unpublished data). 16:0-22:6PE/SM (1:1) (Fig. 3 *d*) shows two distinct exotherms with $T_m = 8$ and 24°C. We attribute them, respectively, to transitions for 16:0-22:6PE-rich/SM-poor and 16:0-22:6PE-poor/SM-rich phases. The T_m value for the 16:0-22:6PE-rich/SM-poor phase coincides with the temperature of the transition identified on the basis of spectral moments for 16:0-22:6PE-d_{31}/SM (1:1) (Fig. 3 *b*). Addition of equimolar CHOL to 16:0-18:1PE/SM (1:1) and 16:0-22:6PE/SM (1:1) eliminates all of the transitions seen in the absence of the sterol by DSC.

Equimolar CHOL increases the order of 16:0-18:1PE-d_{31} in 16:0-18:1PE-d_{31}/SM (1:1) more than 16:0-22:6PE-d_{31} in 16:0-22:6PE-d_{31}/SM (1:1) bilayers

The differential effect of adding equimolar CHOL on 16:0-18:1PE-d_{31}/SM (1:1) versus 16:0-22:6PE-d_{31}/SM (1:1) bilayers in the liquid crystalline phase is clear upon examination of the plot of M_1 values against temperature in Fig. 3 (*a* and *b*). We specifically compared the ordering effect of CHOL on 16:0-18:1PE-d_{31}/SM (1:1) versus 16:0-22:6PE-d_{31}/SM (1:1) at 40°C. Table 1 summarizes the first moment M_1 and the average order parameter $\overline{S}_{CD}$ calculated from M_1 via Eq. 2 for all four of the lipid combinations at 40°C. Addition of equimolar CHOL to 16:0-18:1PE-d_{31}/SM (1:1) results in an increase in $\overline{S}_{CD}$ for 16:0-18:1PE-d_{31} by 61%, whereas the change in $\overline{S}_{CD}$ for 16:0-22:6PE-d_{31}/SM/CHOL (1:1:1) compared to 16:0-22:6PE-d_{31}/SM (1:1) bilayers is ~26%. Although these values represent a population-weighted average over all coexisting environments between which the deuterated PE molecules exchange, greater interaction of the sterol with the OA- than the DHA-containing PE may be unambiguously inferred.

The ^{2}H NMR spectra at 40°C (Figs. 1 and 2) were FFT depaked to enhance spectral resolution (McCabe and Wassall, 1997). Application of the algorithm produces a spectrum that is equivalent to the spectrum that would be obtained for a planar membrane with the bilayer normal

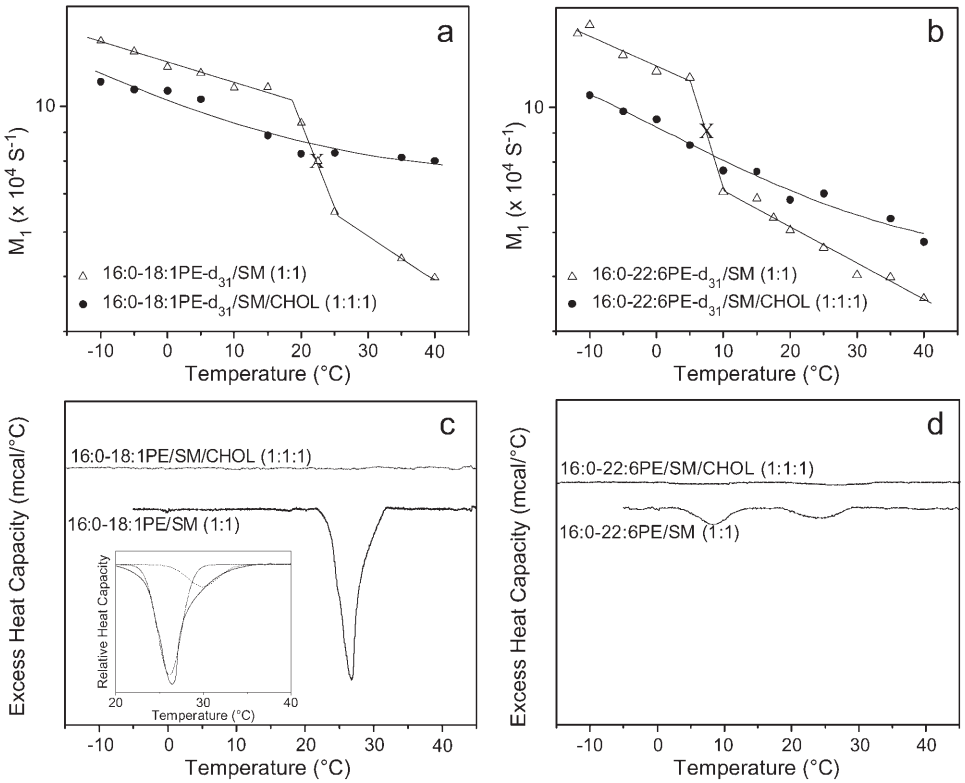

FIGURE 3 (*a* and *b*) Variation in the first moment M_1 (Eq. 1) as a function of temperature for bilayers of (*a*) 16:0-18:1PE-d_{31}/SM (1:1) and 16:0-18:1PE-d_{31}/SM/CHOL (1:1:1), and (*b*) 16:0-22:6PE-d_{31}/SM (1:1) and 16:0-22:6PE-d_{31}/SM/CHOL (1:1:1). M_1 is plotted logarithmically and values have a ±2% error. The transition temperature T_m, designated by X, is the midpoint of the sharp drop in moment that accompanies the chain-melting transition. (*c* and *d*) Corresponding DSC cooling scans for (*c*) 16:0-18:1PE/SM (1:1) and 16:0-18:1PE/SM/CHOL (1:1:1), and (*d*) 16:0-22:6PE/SM (1:1) and 16:0-22:6PE/SM/CHOL (1:1:1). The scans with cholesterol are slightly offset along the excess heat capacity axis to aid observation. The inset is a high-resolution deconvolution of the DSC cooling scan for 16:0-18:1PE/SM (1:1). The dotted and dashed lines represent the 16:0-18:1PE-rich and SM-rich phases, respectively.

parallel to the magnetic field (Fig. 4). They possess an outermost composite doublet, representing ordered methylenes in the upper part of the acyl chain, and five to six well-resolved doublets corresponding to the methylenes and terminal methyl that display progressively less order in the lower portion of the *sn*-1 acyl chain. The depaked data were utilized to calculate profiles of order parameter S_{CD} along the perdeuterated *sn*-1 chain of the PE component in the lipid mixtures (Fig. 5). The smoothed profiles were created by assigning equal integrated intensity to each methylene group and a monotonic decrease in order toward the terminal methyl was assumed (Lafleur et al., 1989). Fig. 5 illustrates order parameters as a function of acyl chain carbon position for bilayers of 16:0-18:1PE-d_{31}/SM (1:1) (Fig. 5 *a*) and 16:0-22:6PE-d_{31}/SM (1:1) (Fig. 5 *b*) in the absence or presence of equimolar CHOL at 40°C. A similar qualitative trend is observed for all four of the order parameter profiles. The upper part of the perdeuterated palmitoyl chains is marked by a plateau region of approximately constant order with a subsequent decrease in order toward the bottom of the chains. In agreement with the average order parameters $\overline{S}_{CD}$ listed in Table 1, addition of CHOL to both phospholipid mixtures results in ordering of the acyl chains at all carbon positions. CHOL's ordering effect is most pronounced in the plateau region toward the top of the perdeuterated acyl chain for both 16:0-18:1PE-d_{31} and 16:0-22:6PE-d_{31} as opposed to the middle of the bilayers. At carbon position 2, for instance, the value of S_{CD} changes from ~0.24 to ~0.37 for 16:0-18:1PE-d_{31}/SM (1:1), and for 16:0-22:6PE-d_{31}/SM (1:1) shows a smaller change ~0.24 to ~0.32. The respective differences in S_{CD} correspond to a sterol-induced increase of 54.2 and 33.3%. This differential in the effect of CHOL on the OA- and DHA-containing mixtures is consistent with the calculated changes in $\overline{S}_{CD}$ reported in Table 1.

TABLE 1 Data derived from ^{2}H NMR studies of 16:0-18:1PE-d_{31}/SM (1:1) or 16:0-22:6PE-d_{31}/SM (1:1) in the absence or presence of equimolar CHOL at 40°C

Lipid composition	M_1 (10^4 s^{-1})	$\overline{S}_{CD}$	Increase in order due to CHOL
16:0-18:1PE-d_{31}/SM (1:1)	4.98	0.163	
16:0-18:1PE-d_{31}/SM/CHOL (1:1:1)	8.01	0.263	61%
16:0-22:6PE-d_{31}/SM (1:1)	4.58	0.150	
16:0-22:6PE-d_{31}/SM/CHOL (1:1:1)	5.77	0.189	26%

AFM measurements demonstrate differences in phase separation between 16:0-18:1PE/SM/CHOL (1:1:1) vs. 16:0-22:6PE/SM/CHOL (1:1:1)

AFM is a useful tool for assessing phase separations in supported bilayers. The AFM measurements reported here are a preliminary attempt to relate the differences in phase separation seen spectroscopically by NMR with lateral organization. Fig. 6 presents AFM images of 16:0-18:1PE/

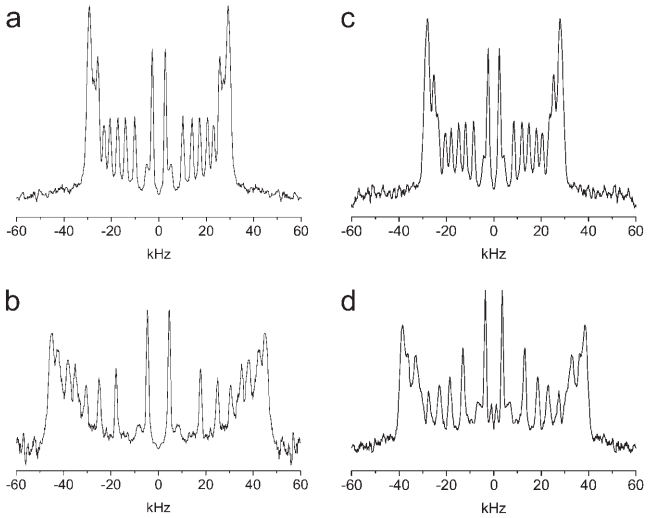

FIGURE 4 FFT depaked spectra for (*a*) 16:0-18:1PE-d_{31}/SM (1:1); (*b*) 16:0-18:1PE-d_{31}/SM/CHOL (1:1:1); (*c*) 16:0-22:6PE-d_{31}/SM (1:1); and (*d*) 16:0-22:6PE-d_{31}/SM/CHOL (1:1:1) at 40°C.

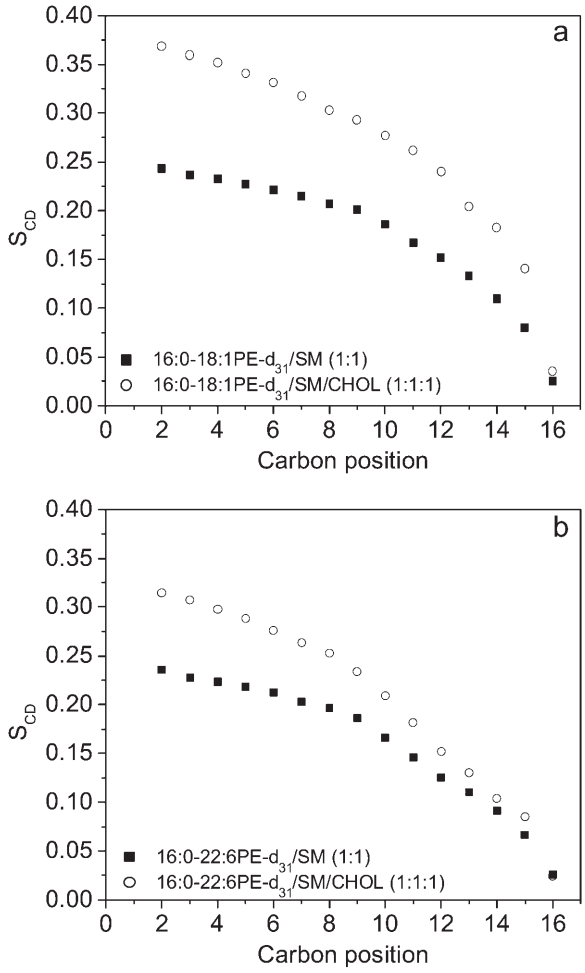

FIGURE 5 Smoothed order parameter profiles generated from depaked spectra at 40°C for bilayers of (*a*) 16:0-18:1PE-d_{31}/SM (1:1) and 16:0-18:1PE-d_{31}/SM/CHOL (1:1:1), and (*b*) 16:0-22:6PE-d_{31}/SM (1:1) and 16:0-22:6PE-d_{31}/SM/CHOL (1:1:1).

SM/CHOL (1:1:1) and 16:0-22:6PE/SM/CHOL (1:1:1) supported bilayers on mica obtained at room temperature in the lamellar liquid crystalline phase. Visual inspection clearly reveals differences in the topology of the two lipid mixtures. For both samples, the thicker (lighter) patches are assigned to SM-rich or SM/CHOL-rich domains whereas the thinner (darker) regions are assigned to PE-rich phases. The former regions extend above the latter on average by 1.1 ± 0.1 nm (Fig. 6, *insets*). The SM-rich or SM/CHOL-rich domains were identified based upon varying the amount of SM or SM/CHOL in our lipid mixtures (data not shown). In the case of 16:0-18:1PE/SM/CHOL, the lighter domains comprise 26 ± 2% of the total bilayer surface (Fig. 6, *top*) whereas 59 ± 10% of the total bilayer surface was covered by lighter domains in the 16:0-22:6PE/SM/CHOL (1:1:1) bilayers (Fig. 6, *bottom*), demonstrating greater phase separation with the DHA-containing phospholipid. In all images taken it was evident that domains observed in the 16:0-22:6PE/SM/CHOL (1:1:1) bilayers were very large (>1 μm in size) and interconnected compared to those (<1 μm in size) observed in the 16:0-18:1PE/SM/CHOL (1:1:1) membranes. The connected nature of the raft domains in the DHA-containing membranes, often extending beyond the image field, made comparison of raft size between the two model membranes uncertain. Vesicles that did not fuse appear as bright spots on the images and are eliminated in the calculations. There was a variation of 0.5–0.6 nm in bilayer thickness for the two model membranes that was determined by measuring the height difference from the exposed mica holes or from the edges of the bilayers. Giocondi et al. (2004) suggested that changes in bilayer thickness from sample to sample measured in this manner can be attributed to differences in the hydration layer between the substrate and bilayers. In a few places, the heights of some phase-separated domains could be up to 2.4 nm above the background bilayer. These structures, called ''corrugated domains,'' have been reported by others in similar AFM studies (Giocondi et al., 2004) but were not included in our calculations.

16:0-18:1PE is less detergent-soluble than 16:0-22:6PE in the presence of equimolar SM/CHOL in lipid vesicles

The detergent extraction method is widely utilized to assess the presence of lipid microdomains in membranes and in fact is a hallmark of lipid rafts (Edidin, 2003b). We compared solubilization of MLVs composed of 16:0-18:1PE/SM/CHOL (1:1:1) versus 16:0-22:6PE/SM/CHOL (1:1:1) to assess differences in phase separation between the OA- and DHA-containing PEs with the lipid-raft molecules SM and CHOL. Detergent-resistant studies were performed at 4°C,

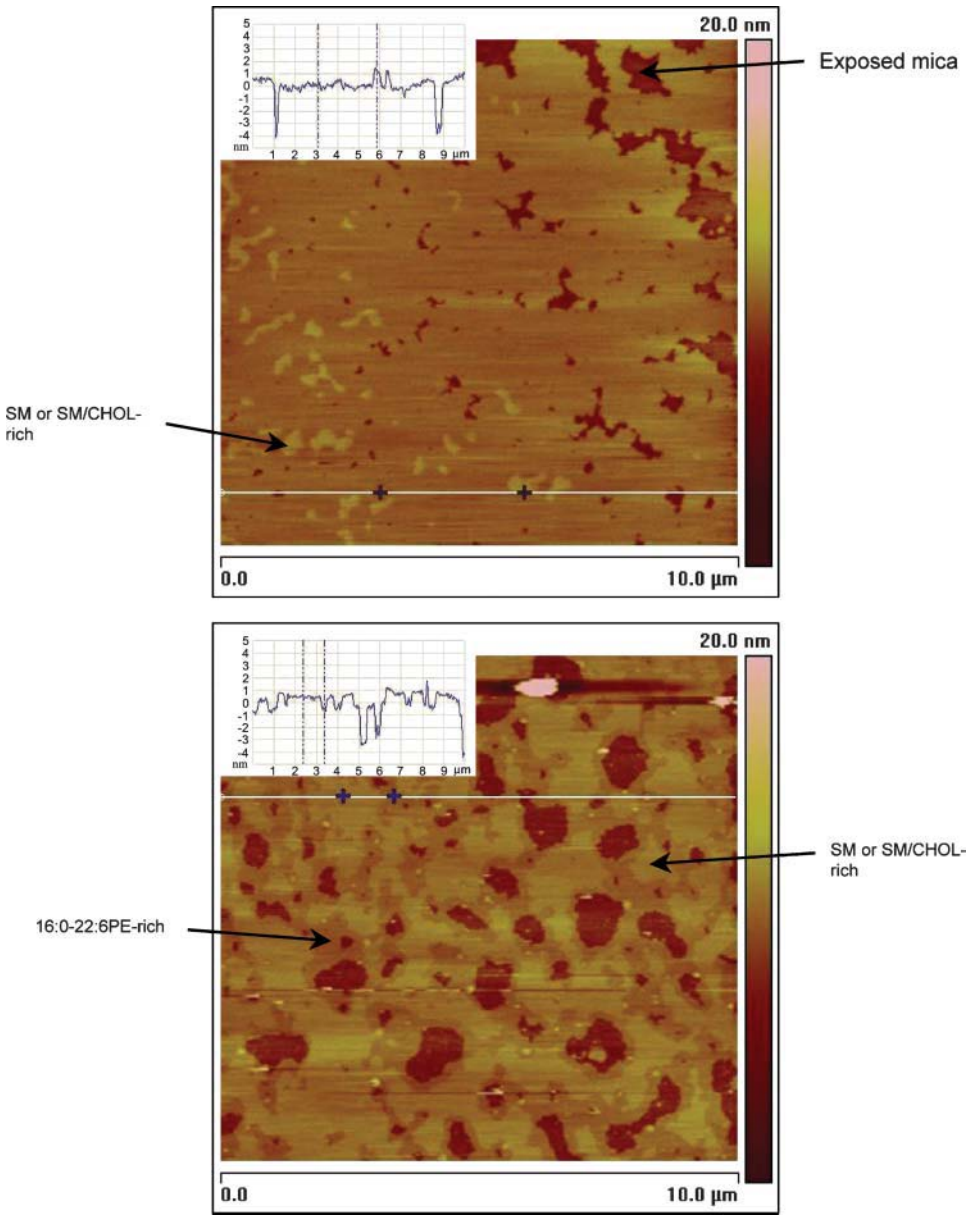

FIGURE 6 Representative AFM images at 23°C of 16:0-18:1PE/SM/CHOL (1:1:1) (*top*) and 16:0-22:6PE/SM/CHOL (1:1:1) (*bottom*) supported bilayers with a *z* scale of 20 nm (*color bar*). The insets present the section profile corresponding to the white line on the image.

where most detergent solubility experiments have been conducted, and at 40°C to approximately mimic physiological temperature. Fig. 7 shows the percentage of lipid found in the detergent-soluble fraction relative to the total amount of that lipid in the vesicles. Results are presented as the average + standard deviation (SD) from three separate experiments consisting of a minimum of four samples. Less than 10% of SM or CHOL are found in the soluble fractions for both 16:0-18:1PE/SM/CHOL (1:1:1) and 16:0-22:6PE/SM/CHOL (1:1:1) mixtures at 4°C (Fig. 7 *a*), which agrees with the notion that these lipids are detergent-resistant. Increasing the temperature to 40°C results in a higher percentage of SM and CHOL in the DSM fractions for both samples (Fig. 7 *b*). The change is greatest for CHOL in 16:0-22:6PE/SM/CHOL (1:1:1) where ~30% CHOL is detergent-solubilized but, nevertheless, SM and CHOL predominantly remain detergent-resistant. An increase in solubilization of SM/CHOL at higher temperature has been reported by others (Gandhavadi et al., 2002). Most notably, we observe that a significant difference exists in the percentage of 16:0-18:1PE versus 16:0-22:6PE species found in the DSM fractions at both temperatures. Whereas the majority of the monounsaturated phospholipid is detergent-insoluble, the opposite is true for the polyunsaturated PE. At 4°C, ~22% 16:0-18:1PE in contrast to ~70% 16:0-22:6PE is found in the soluble fraction, demonstrating a threefold difference in phase separation between the two PE lipids (Fig. 7 *a*). At 40°C, the differential is nearly twofold, with ~40% of the 16:0-18:1PE and ~78% of the 16:0-22:6PE species located in the detergent-soluble

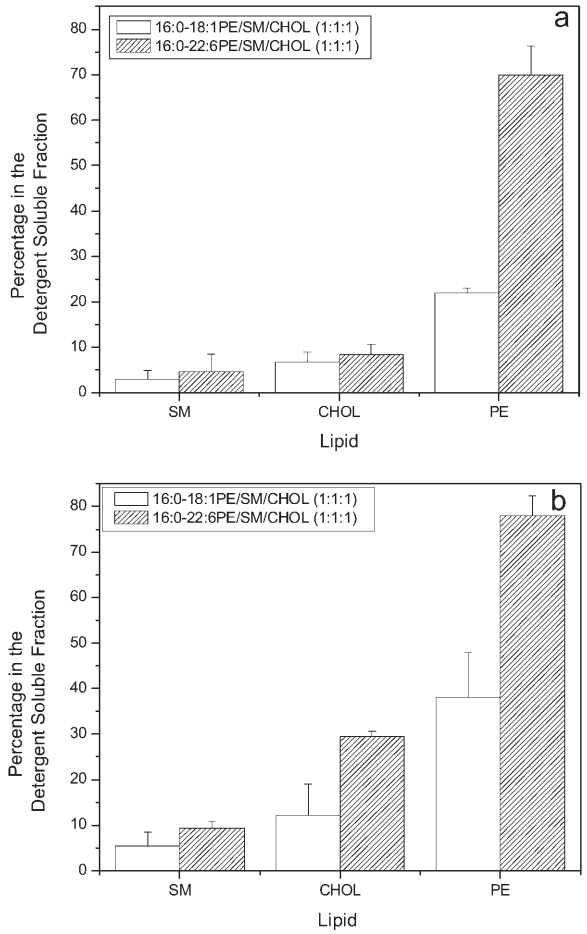

FIGURE 7 Percentage (mean + SD) of SM, CHOL, and PE found in the DSM fraction of Triton X-100 treated aqueous multilamellar dispersions of 16:0-18:1PE/SM/CHOL (1:1:1) (*no pattern*) or 16:0-22:6PE/SM/CHOL (1:1:1) (*dense pattern*) at (*a*) 4 and (*b*) 40°C. Each value is relative to the total amount of the specific lipid in both detergent-soluble and detergent-insoluble fractions. The values represent a minimum of four samples from three separate experiments. Supernatant lipids were recovered by HPTLC and quantified via charring (Materials and Methods).

fractions (Fig. 7 *b*). Increasing the temperature results in greater solubilization of both PE lipids as is the case with SM and CHOL.

OA and DHA are mostly detergent-solubilized in cells

We utilized detergent-resistant assays with neonatal cardiomyocytes to look for differences in the localization (raft versus non-raft) of OA and DHA in a cellular system. Sucrose gradients were collected in 1-mL increments (top to bottom) and fractions 4–6 are denoted as the DRM raft-rich fractions based on binding of β-cholera toxin to the raft marker GM1 (Fig. 8 *a*). We specifically assessed differences in the localization of [^{3}H]OA (Fig. 8 *b*) and [^{14}C]DHA (Fig. 8 *a*) in neonatal cardiomyocytes. It is important to note that

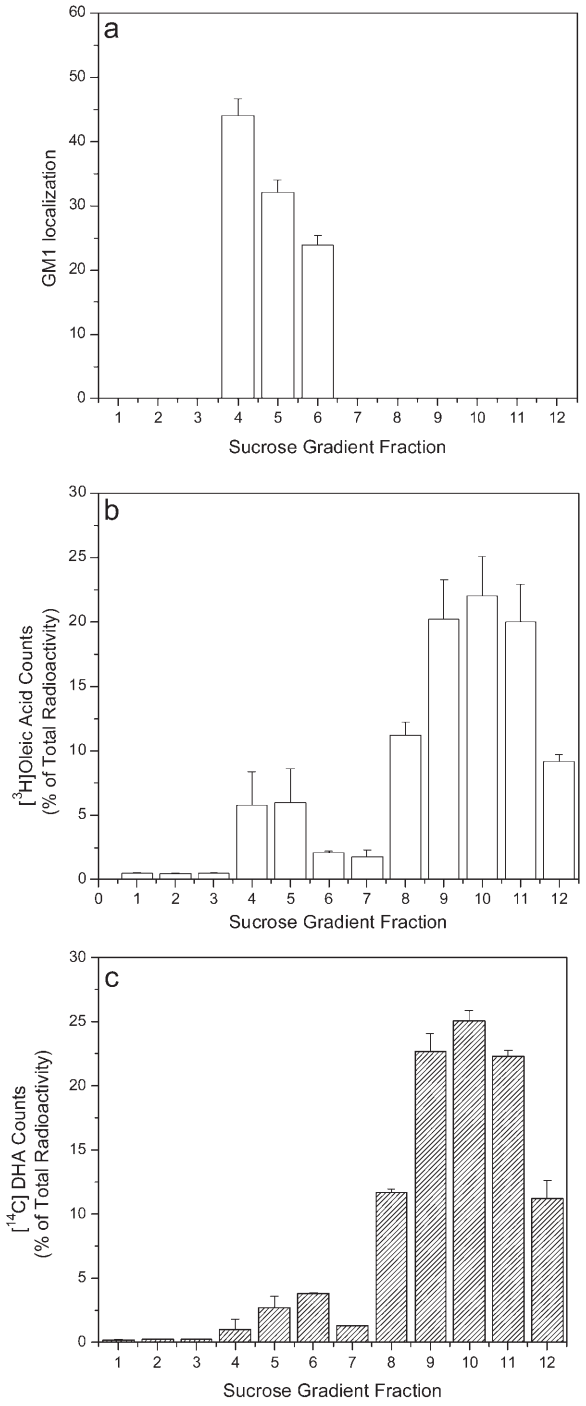

FIGURE 8 Percentage (mean + SD) of (*a*) GM1, (*b*) [^{3}H]OA, and (*c*) [^{14}C]DHA in sucrose-gradient fractions of neonatal cardiomyocytes. Cells were incubated at 4°C in the presence of 1% Triton X-100, homogenized, and placed on a 5–40% sucrose gradient. After ultracentrifugation, fractions were collected in 1-mL increments from the top to bottom of the centrifuge tubes and analyzed (Materials and Methods). Values represent a minimum of three separate experiments.

most of the [^{3}H]OA and [^{14}C]DHA was found in the non-raft DSM fractions 8–12. Nevertheless, a significant difference exists between the percentage of each fatty acid found in the DRM fractions. In the case of [^{3}H]OA, 14.5 ± 2.6% of the radiolabel was found in the DRM fractions. In comparison, 7.4 ± 0.9% of the [^{14}C]DHA was located in the DRM fractions, demonstrating a nearly twofold difference between the monounsaturated and polyunsaturated fatty acids. Although incorporation of free fatty acids into phospholipids with this method is well characterized (Munro, 2003; Stulnig et al., 1998), we verified incorporation of radiolabeled OA and DHA into phospholipids using HPTLC analysis. Most of the OA and DHA were incorporated into PCs and PEs with lesser amounts into other phospholipids (data not shown).

DISCUSSION

We have previously suggested that polyunsaturation may trigger lipid phase separations affecting lipid raft structure and function (Shaikh et al., 2002). The focus of this study was to further assess the effect of replacing a phospholipid-containing OA with the beneficial ω-3 fatty acid DHA on raft molecules. We examined phase behavior and molecular organization in 16:0-18:1PE-d_{31}/SM/CHOL (1:1:1) versus 16:0-22:6PE-d_{31}/SM/CHOL (1:1:1) model bilayer membranes using ^{2}H NMR spectroscopy, DSC, AFM, and detergent extractions. In addition, we evaluated differences in phase separation of OA versus DHA from rafts using the biochemical detergent extraction method in cells.

Role of steric incompatibility between CHOL and DHA

^{2}H NMR indicates cholesterol interacts less with 16:0-22:6PE-d_{31} than 16:0-18:1PE-d_{31} in SM-containing mixtures. Spectral moments evaluated at 40°C upon the incorporation of CHOL into 16:0-18:1PE-d_{31}/SM (1:1) and 16:0-22:6PE-d_{31}/SM (1:1) membranes translate to increases of ~61% and ~26%, respectively, in order (Table 1). We recently established a reduced affinity of CHOL for 16:0-22:6PE in comparison to 16:0-18:1PE in the absence of SM (Shaikh et al., 2003a). First moments derived from ^{2}H NMR spectra revealed that adding equimolar CHOL to 16:0-18:1PE-d_{31} broadened the T_m until it became unobservable. In contrast, the transition was detected in 16:0-22:6PE-d_{31}/CHOL (1:1) and was relatively unperturbed relative to when sterol was absent. Corroborating x-ray diffraction experiments found a solubility of 32 ± 3 mol % for CHOL in 16:0-22:6PE membranes whereas 51 ± 3 mol % could be accommodated in 16:0-18:1PE (Shaikh et al., 2003a). Thus, steric incompatibility between CHOL and the highly disordered PUFA chain in 16:0-22:6PE may serve as a molecular mechanism by which lateral phase separations into l_o and l_d microdomains are promoted.

Evidence for unfavorable interactions between DHA-containing phospholipids and CHOL has been reported in other model systems as well. Demel et al. (1972) and later Zerouga et al. (1995) demonstrated weak association between a DHA-containing PC and CHOL based upon percent condensation calculated for monolayers at the air-water interface. Additional support for a reduced affinity between CHOL and DHA-containing phospholipids has come from a bilayer study by Huster et al. (1998) indicating that CHOL maintains a closer contact with saturated acyl chains in heteroacid *sn*-1 saturated *sn*-2 polyunsaturated phospholipids. These researchers showed by two-dimensional NOESY ^{1}H NMR spectroscopy with magic angle spinning that the sterol displays higher chain-to-cholesterol cross-relaxation rates with saturated chains than with polyunsaturated chains in mixed 18:0-22:6PC/CHOL bilayers, suggesting preferential interaction between CHOL and the saturated 18:0 *sn*-1 chain (Huster et al., 1998). By a combination of solid-state ^{2}H NMR and x-ray diffraction techniques we have also demonstrated low sterol solubility in PC and PE membranes containing PUFAs (Brzustowicz et al., 1999, 2002a,b; Shaikh et al., 2003a).

CHOL-OA interactions

Our ^{2}H NMR data, on the contrary, give no indication that 16:0-18:1PE has a low degree of affinity for cholesterol. The increase of ~61% in average order parameter $\overline{S}_{CD}$ upon the introduction of equimolar cholesterol into 16:0-18:1PE-d_{31}/SM (1:1) bilayers (Table 1), furthermore, is greater than we saw in 16:0-18:1PE-d_{31} bilayers where $\overline{S}_{CD}$ rose by 33% (Shaikh et al, 2003a). The implication is that the OA-containing PE does not phase separate well from the lipid-raft molecules SM and CHOL in the 16:0-18:1PE/SM/CHOL (1:1:1) system compared to 16:0-22:6PE/SM/CHOL (1:1:1). This conclusion regarding 16:0-18:1PE may reflect the dependence upon composition and temperature found by others for lateral segregation into domains in PC/SM/CHOL mixtures (de Almeida et al., 2003; Veatch and Keller, 2003). A DSC and AFM study by Milhiet et al. (2002) found no evidence for domains at $\chi_{CHOL} \geq 0.33$ in 16:0-18:1PC/SM (3:1) bilayers although phase separation was observed at $\chi_{CHOL} \leq 0.33$. As we examined only a single CHOL content here, phase separation between 16:0-18:1PE and SM/CHOL domains may be possible at lower CHOL concentrations or at different 16:0-18:1PE/SM ratios. In the absence of CHOL, the deconvolution of the exotherm in our DSC scans into two components does suggest that phospholipid and sphingolipid phase separate in 16:0-18:1PE/SM (1:1) (Fig. 3 *c*, *inset*). A recent solid-state NMR investigation concluded that 16:0-18:1PC does not phase separate from SM/CHOL raft domains (Aussenac et al., 2003). These researchers found that order parameters for ^{2}H-labeled CHOL in 16:0-18:1PC/SM/CHOL (1:1:1) were between those of 16:0-18:1PC/CHOL (1:1) and SM/CHOL (1:1), implying that the sterol is in

intimate contact with both 16:0-18:1PC and SM in the mixed membrane. Explanations include homogeneous mixing and fast exchange of labeled cholesterol between 16:0-18:1PC/CHOL and SM/CHOL microdomains. A higher partition coefficient of CHOL in an OA-containing PC in comparison to a DHA-containing PC was also recently reported. Using a novel vesicle-cyclodextrin system to measure CHOL's partition coefficient in unilamellar vesicles, Niu and Litman (2002) measured a 2.6-fold higher partitioning of CHOL in 16:0-18:1PC compared to 16:0-22:6PC.

Phase separation observed with AFM

Our AFM results with 16:0-18:1PE/SM/CHOL (1:1:1) show that most of the bilayer is homogeneous in thickness with a few (~26% of the total surface area) phase-separated domains rich in SM or SM/CHOL (Fig. 6). We propose that CHOL interacts with both SM and 16:0-18:1PE, which results in a homogenous l_o phase with a few SM- or SM/CHOL-rich light domains protruding from the bilayer surface. This finding is consistent with our ^{2}H NMR and detergent-resistant observations that CHOL interacts strongly with 16:0-18:1PE-d_{31} in the presence of equimolar SM. In addition, ^{2}H NMR studies have shown that 16:0-18:1PE/CHOL can form an l_o phase (Pare and Lafleur, 1998). In the case of 16:0-22:6PE/SM/CHOL (1:1:1) bilayers (Fig. 6), more phase-separated light (SM- or SM/CHOL-rich) domains are observed (~59% of the total surface area). The dark thinner domains are attributed to the l_d phase rich in 16:0-22:6PE. Again, this finding is consistent with our ^{2}H NMR and detergent-resistant data that suggest enhanced phase separation in the presence of polyunsaturation. A continuing problem in membrane structural studies is determining the actual size of lipid domains. Although our earlier NMR work on mixed PCs is consistent with diffusion-mediated fast exchange of cholesterol between microdomains <160 Å in size (Brzustowicz et al., 2002b), our AFM measurements here identify domains in the micron range. Any attempt to reconcile this apparent discrepancy must take into account that, due to very different timescales, the two methods are inherently sensitive to inequivalent length scales. The timescale of the ^{2}H NMR approach is $\sim 10^{-5}$ s, whereas AFM is much slower. Our AFM images were obtained in ~2 min, during which time lateral diffusion of lipid would prevent observation of individual microdomains. One possible explanation that we are pursuing is that the very large domains observed with AFM are actually composed of clusters of much smaller domains implied by NMR.

Detergent-solubilization studies in vesicles

Detergent-solubilization studies were conducted at 4 and 40°C to further evaluate phase separations in our model membrane systems. They were undertaken at higher and lower temperature because the validity of detergent extractions that are routinely performed at 4°C to assess phase separation has been questioned and may not reflect the phase state of the lipid mixture at physiological temperature (Shogomori and Brown, 2003). However, our ^{2}H NMR and DSC data for 16:0-18:1PE/SM/CHOL (1:1:1) and 16:0-22:6PE/SM/CHOL (1:1:1) (Figs. 2 and 3) establish that each mixture is liquid crystalline at both low and high temperatures. The results identify that ~60–80% 16:0-18:1PE versus ~20–30% 16:0-22:6PE are found in the DRM fraction at either 4 or 40°C (Fig. 7). Although it is plausible that Triton may be inducing domain formation (Heerklotz, 2002), our detergent extraction finding is in agreement with our NMR observation that CHOL increases the order of both PEs in the presence of SM but exerts much greater effect on 16:0-18:1PE-d_{31} than on 16:0-22:6PE-d_{31} (Table 1 and Fig. 3). The significant difference in the amount of 16:0-18:1PE in the DSM fraction compared to 16:0-22:6PE for both temperatures, moreover, suggests phase separation that is driven by the presence of the polyunsaturated acyl chain in agreement with our AFM data. The differences in phase separation are also correlated to the differences in T_m of the two PEs examined, in accord with previous findings (Ferguson, 1999; Shaikh et al., 2003b). Phase separation driven by the presence of acyl chain unsaturation, as assessed by detergent extraction, was identified in an 18:1-18:1PC/SM/CHOL (1:1:1) model system by McIntosh and coworkers (Gandhavadi et al., 2002; McIntosh et al., 2003). These researchers saw a greater proportion of 18:1-18:1PC in the DSM fraction at 4 and 37°C in the presence of equimolar SM and CHOL, and suggested that mechanical properties of DRMs and DSMs may have implications for peptide sorting (McIntosh et al., 2003).

Detergent-solubilization studies in cells

As seen in our model membrane studies, a significant difference in the amount of OA versus DHA was found in DRM fractions isolated from cardiomyocytes. However, our cellular studies reveal that the vast majority of OA and DHA are localized in the DSMs, whereas our model membrane studies would predict that most of the OA would be raft-localized in cells. This inconsistency suggests that our model membrane studies do not correlate perfectly with our cellular model. Perhaps a three-component lipid system does not realistically reflect the complex heterogeneities that may arise in the plasma membrane due to interactions amongst various lipids, proteins, and even the cytoskeleton. Although this supposition has validity, we believe that the discrepancy in the OA data between model membranes and cells can be explained better if one takes into account the limitations of the detergent extraction approach. Lipid phase behavior is highly temperature-dependent and complicated in a real cell membrane that is composed of hundreds of different lipid molecular species. Thus, the reduction in temperature could have resulted in changes in lipid organization that would be

difficult to model in simple two- or three-component vesicles. A recent study by Schuck et al. (2003) furthermore showed that different detergents show considerable differences in their ability to solubilize membrane lipids and proteins. This underscores the difficulty of interpreting detergent extractions as a tool for understanding membrane organization. These researchers suggested that the presence of certain lipids or proteins in the DRM fraction does not necessarily indicate an association with the same microdomain in the biological membrane (Schuck et al., 2003). Another major limitation of the detergent-solubilization technique is that partial solubilization may not be the result of differences in solubility between microdomains but rather due to differences in the solubility of the two leaflets. Perhaps OA and DHA are localizing to different leaflets. Indeed Knapp et al. (1994) reported that DHA is preferentially accepted into the inner leaflet of PEs and phosphatidylserines of the erythrocyte plasma membrane. Further investigation into this matter is clearly of interest. Finally, different cell lines may show different results. We examined changes in OA and DHA localization in MDA-MB-231 breast cancer cells where differences were smaller than those reported for cardiomyocytes (Shaikh et al., unpublished data).

Physiological relevance of DHA-lipid raft phase separations

Since ω-3 fatty acids are increasingly being utilized clinically as adjuvant immunosuppressants in the treatment of inflammatory diseases, it is becoming evident that PUFAs modulate immune responses by suppressing T-cell activation in lymphoid cells. The suggestion has been made that inhibition of T-cell signaling may be mediated by modification of lipid raft microdomains upon incorporation of various PUFAs including eicosapentaenoic acid (20:5) and arachidonic acid (20:4) (Webb et al., 2000; Zeyda et al., 2002). Although relatively little is known about the molecular interactions between PUFAs and lipid rafts, a few studies have emerged to explain the physiological importance of the PUFA-lipid raft relationship at a cellular level.

A recent investigation showed that acylated proteins found in lipid rafts were displaced due to the incorporation of eicosapentaenoic acid in Jurkat T cells (Stulnig et al., 2001). In another study, it was demonstrated that DHA stimulates phospholipase D1 activity in stimulated human peripheral blood mononuclear cells, which may be responsible for some of the DHA-induced immunosuppression (Diaz et al., 2002). These researchers found that phospholipase D1 (PLD1), located in the DRM fractions of sucrose gradients, is lipid raft-localized in the absence of DHA treatment and that its activity is impaired (Diaz et al., 2002). Treatment of the peripheral blood mononuclear cells with DHA resulted in changing its localization from DRMs to DSMs and an increase in activity was observed. Both studies have suggested that altered lipid raft formation may be responsible for the known inhibitory effects of PUFAs on T-cell activation. However, the molecular mechanism by which this occurs remains elusive.

In Fig. 9 we present a cartoon depiction of the molecular mechanism by which activity of proteins such as PLD1 may change upon incorporation of DHA into cells. We hypothesize that incorporation of a DHA-phospholipid results in enhanced phase separation of the l_d-favoring, DHA-rich phospholipids from the l_o lipid rafts, thereby changing the localization and activity of selected proteins. Phase separation is proposed to be triggered by the decreased solubility of CHOL in DHA-containing phospholipids (Brzustowicz et al., 2002a; Shaikh et al., 2003a). In the example depicted in Fig. 9, as the DHA-phospholipid accumulates into the nonraft domain, CHOL is driven to the raft domain. The protein X, originally located in a raft where it is inactive, then partitions into the nonraft, DHA-rich domain where its conformation is altered resulting in enhanced activity. An example of a protein that may follow this path is PLD1 that upon DHA treatment is excluded from rafts. The accumulation of PLD1 in DHA-rich, nonraft domains activates the protein and disrupts signal transduction events, accounting for the fatty acid's known immunosuppressive effects. DHA has also been implicated in influencing the activity of other proteins including rhodopsin (Litman and Mitchell, 1996), protein kinase C (Padma and Das, 1999), phospholipase C (Sanderson and Calder, 1998), insulin receptor (McCallum and Epand, 1995), gamma-aminobutyric type A receptor (Nabekura et al., 1998), and the nicotinic acetylcholine receptor (Rankin et al., 1997).

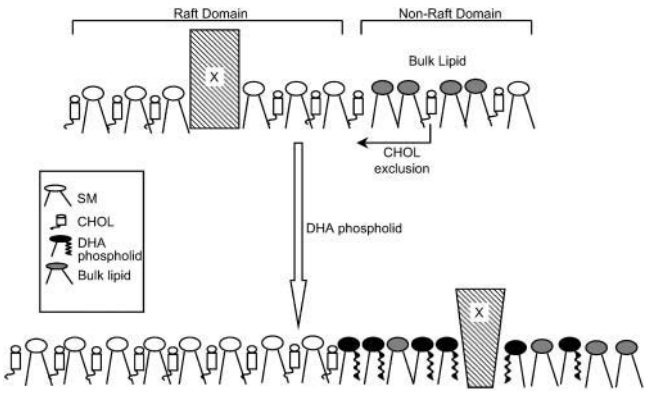

FIGURE 9 Cartoon depiction of DHA-induced alteration of plasma membrane lipid domain structure. The outer membrane leaflet is shown since it is here that the SM- and cholesterol-rich l_o (raft) domains exist in a background of nonraft bulk lipids. Upon the addition of a DHA-rich phospholipid, cholesterol is excluded from the nonraft (l_d) domains into the raft domains, increasing raft size and stability. In the example presented here, the inactive protein, X, initially found in the raft domain, is then recruited to the DHA-rich, nonraft domain where it undergoes a conformational change, resulting in its activation.

CONCLUSION

Our results identify major differences in the molecular interactions of OA versus DHA with raft molecules. These findings provide further evidence in support of the hypothesis that DHA-containing phospholipids will phase separate into DHA-rich, SM/CHOL-poor and DHA-poor, SM/CHOL-rich microdomains. Studies of DHA-lipid raft phase separations may contribute to understanding more complex signaling pathways involving proteins. Perhaps DHA exerts its beneficial health effects on numerous disease states including depression, heart disease, various cancers, schizophrenia, and arthritis by influencing lipid raft-mediated cell signaling events.

This work was supported by a grant from the National Institutes of Health (RO1CA57212).

REFERENCES

Ahmed, S. N., D. A. Brown, and E. London. 1997. On the origin of sphingolipid/cholesterol-rich detergent insoluble cell membranes: physiological concentrations of cholesterol and sphingolipid induce formation of a detergent-insoluble, liquid-ordered lipid phase in model membranes. *Biochemistry.* 36:10944–10953.

Aussenac, F., M. Tavares, and E. J. Dufourc. 2003. Cholesterol dynamics in membranes of raft composition: a molecular point of view from 2H and 31P solid-state NMR. *Biochemistry.* 42:1383–1390.

Brown, D. A., and E. London. 2000. Structure and function of sphingolipid and cholesterol-rich membrane rafts. *J. Biol. Chem.* 275:17221–17224.

Brzustowicz, M. R., V. Cherezov, M. Caffrey, W. Stillwell, and S. R. Wassall. 2002b. Molecular organization of cholesterol in polyunsaturated membranes: microdomain formation. *Biophys. J.* 82:285–298.

Brzustowicz, M. R., V. Cherezov, M. Zerouga, M. Caffrey, W. Stillwell, and S. R. Wassall. 2002a. Controlling membrane cholesterol content. A role for polyunsaturated (docosahexaenoate) phospholipids. *Biochemistry.* 41:12509–12519.

Brzustowicz, M. R., W. Stillwell, and S. R. Wassall. 1999. Molecular organization of cholesterol in polyunsaturated phospholipid membranes: a solid state 2H NMR investigation. *FEBS Lett.* 451:197–202.

Davis, J. H. 1983. The description of membrane lipid conformation, order and dynamics by 2H-NMR. *Biochim. Biophys. Acta.* 737:117–171.

de Almeida, R. F. M., A. Fedorov, and M. Prieto. 2003. Sphingomyelin/phosphatidylcholine/cholesterol phase diagram: boundaries and composition of lipid rafts. *Biophys. J.* 85:2406–2416.

Demel, R. A., W. S. M. Geurts van Kessel, and L. L. M. van Deenen. 1972. The properties of polyunsaturated lecithins in monolayers and liposomes and the interactions of these lecithins with cholesterol. *Biochim. Biophys. Acta.* 266:26–40.

Diaz, O., A. Berquand, M. Dubois, S. Di Agostino, C.C. Sette, S. Bourgoin, M. Lagarde, G. Nemoz, and A.-F. Prigent. 2002. The mechanism of docosahexaenoic acid-induced phospholipase D activation in human lymphocytes involves exclusion of the enzyme from lipid rafts. *J. Biol. Chem.* 277:39368–39378.

Edidin, M. 1993. Patches and fences: probing for plasma membrane domains. *J. Cell Sci.* 17:165–169.

Edidin, M. 2003a. Lipids on the frontier: a century of cell-membrane bilayers. *Nat. Rev. Mol. Cell Biol.* 4:414–418.

Edidin, M. 2003b. The state of lipid rafts: from model membranes to cells. *Annu. Rev. Biophys. Biomol. Struct.* 32:257–283.

Eldho, N. V., S. E. Feller, S. Tristram-Nagle, I. V. Polozov, and K. Gawrisch. 2003. Polyunsaturated docosahexaenoic vs docosapentaenoic acid—differences in lipid matrix properties from the loss of one double bond. *J. Am. Chem. Soc.* 125:6409–6421.

Ferguson, M. A. 1999. The structure, biosynthesis and functions of glycosylphosphatidylinositol anchors, and the contributions of trypanosome research. *J. Cell Sci.* 112:2799–2809.

Gandhavadi, M., D. Allende, A. Vidal, S. A. Simon, and T. J. McIntosh. 2002. Structure, composition, and peptide binding properties of detergent-soluble bilayers and detergent resistant rafts. *Biophys. J.* 82:1469–1482.

Giocondi, M.-C., P. E. Milhiet, P. Dosset, and C. L. Grimellec. 2004. Use of cyclodextrin for AFM monitoring of model raft formation. *Biophys. J.* 86:861–869.

Graham, J. M., and J. A. Higgins. 1997. Membrane Analysis. Springer-Verlag, New York.

Heerklotz, H. 2002. Triton promotes domain formation in lipid raft mixtures. *Biophys. J.* 83:2693–2701.

Hooper, N. 1999. Detergent-insoluble glycosphingolipid-rich membrane domains, lipid rafts and caveolae (review). *Mol. Membr. Biol.* 16: 145–156.

Huang, J., J. T. Buboltz, and G. W. Feigenson. 1999. Maximum solubility of cholesterol in phosphatidylcholine and phosphatidylethanolamine bilayers. *Biochim. Biophys. Acta.* 1417:89–100.

Huster, D., K. Arnold, and K. Gawrisch. 1998. Influence of docosahexaenoic acid and cholesterol on lateral lipid organization in phospholipid mixtures. *Biochemistry.* 37:17299–17308.

Jump, D. B. 2002. The biochemistry of n-3 polyunsaturated fatty acids. *J. Biol. Chem.* 277:8755–8758.

Knapp, H., F. Hullin, and N. Salem, Jr. 1994. Asymmetric incorporation of dietary n-3 fatty acids into membrane aminophospholipids of human erythrocytes. *J. Lipid Res.* 35:1283–1291.

Lafleur, M., B. Fine, E. Sternin, P. R. Cullis, and M. Bloom. 1989. Smoothed orientational order profile of lipid bilayers by 2H-nuclear magnetic resonance. *Biophys. J.* 56:1037–1041.

Litman, B. J., and D. C. Mitchell. 1996. A role for phospholipid polyunsaturation in modulating membrane protein function. *Lipids.* 31(Suppl):S193–S197.

McCabe, M. A., G. L. Griffith, W. D. Ehringer, W. Stillwell, and S. R. Wassall. 1994. 2H NMR studies of isomeric w3 and w6 polyunsaturated phospholipid membranes. *Biochemistry.* 33:7203–7210.

McCabe, M. A., and S. R. Wassall. 1997. Rapid deconvolution of NMR powder spectra by weighted fast Fourier transformation. *Solid State Nucl. Mag. Reson.* 10:53–61.

McCallum, C. D., and R. M. Epand. 1995. Insulin receptor autophosphorylation and signaling is altered by modulation of membrane physical properties. *Biochemistry.* 34:1815–1824.

McIntosh, T. J., A. Vidal, and S. A. Simon. 2003. Sorting of lipids and transmembrane peptides between detergent-soluble bilayers and detergent-resistant rafts. *Biophys. J.* 85:1656–1666.

Milhiet, P. E., M. C. Giocondi, and C. L. Grimellec. 2002. Cholesterol is not crucial for the existence of microdomains in kidney-brush border membrane models. *J. Biol. Chem.* 22:875–878.

Mitchell, D. C., and B. J. Litman. 1998. Molecular order and dynamics in bilayers consisting of highly polyunsaturated phospholipids. *Biophys. J.* 74:879–891.

Munro, S. 2003. Lipid rafts: elusive or illusive? *Cell.* 115:377–388.

Nabekura, J., K. Noguchi, M. R. Witt, M. Nielsen, and N. Akaike. 1998. Functional modulation of human recombinant gamma-aminobutyric acid type A receptor by docosahexaenoic acid. *J. Biol. Chem.* 273:11056–11061.

Niu, S. L., and B. J. Litman. 2002. Determination of membrane cholesterol partition coefficient using a lipid vesicle-cyclodextrin binary system: effect of phospholipid acyl chain unsaturation and headgroup composition. *Biophys. J.* 83:3408–3415.

Padma, M., and U. N. Das. 1999. Effect of *cis*-unsaturated fatty acids on the activity of protein kinases and protein phosphorylation in macrophage

tumor (AK-5) cells in vitro. *Prostaglandins Leukot. Essent. Fatty Acids.* 60:55–63.

Pare, C., and M. Lafleur. 1998. Polymorphism of POPE/cholesterol system: A 2H nuclear magnetic resonance and infrared spectroscopic investigation. *Biophys. J.* 74:899–909.

Petrache, H. E., A. Salmon, and M. F. Brown. 2001. Structural properties of docosahexaenoyl phospholipid bilayers investigated by solid-state ^{2}H NMR spectroscopy. *J. Am. Chem. Soc.* 123:12611–12622.

Rankin, S. E., G. H. Addona, M. A. Kloczewiak, B. Bugge, and K. W. Miller. 1997. The cholesterol dependence of activation and fast desensitization of the nicotinic acetylcholine receptor. *Biophys. J.* 73:2446–2455.

Rinia, H. A., J. W. Boots, D.T. Rijkers, R.A. Kik, M.M. Snel, R.A. Demel, J.A. Killian, J.P. van der Eerden, and B. de Kruijff. 2002. Domain formation in phosphatidylcholine bilayers containing transmembrane peptides: specific effects of flanking residues. *Biochemistry.* 41:2814–2824.

Sanderson, P., and P. C. Calder. 1998. Dietary fish oil appears to prevent the activation of phospholipase C-gamma in lymphocytes. *Biochim. Biophys. Acta.* 1392:300–308.

Schroeder, R., E. London, and D. Brown. 1994. Interactions between saturated acyl chains confer detergent resistance on lipids and glycosylphosphatidylinositol (GPI)-anchored proteins: GPI-anchored proteins in liposomes and cells show similar behavior. *Proc. Natl. Acad. Sci. USA.* 91:12130–12134.

Schuck, S., M. Honsho, K. Ekroos, A. Shevchenko, and K. Simons. 2003. Resistance of cell membranes to different detergents. *Proc. Natl. Acad. Sci. USA.* 100:5795–5800.

Shaikh, S. R., M. R. Brzustowicz, N. Gustafson, W. Stillwell, and S. R. Wassall. 2002. Monounsaturated PE does not phase-separate from the lipid raft molecules sphingomyelin and cholesterol: role for polyunsaturation? *Biochemistry.* 41:10593–10602.

Shaikh, S. R., V. Cherezov, M. Caffrey, W. Stillwell, and S. R. Wassall. 2003a. Interaction of cholesterol with a docosahexaenoic acid-containing phosphatidylethanolamine: trigger for microdomain/raft formation? *Biochemistry.* 42:12028–12037.

Shaikh, S. R., A. C. Dumaual, L. J. Jenski, and W. Stillwell. 2001. Lipid phase separation in phospholipid bilayers and monolayers modeling the plasma membrane. *Biochim. Biophys. Acta.* 1512:317–328.

Shaikh, S. R., A. C. Dumaual, D. LoCassio, R. A. Siddiqui, and W. Stillwell. 2003b. Acyl chain unsaturation in PEs modulates phase separation from lipid raft molecules. *Biochem. Biophys. Res. Commun.* 311:793–796.

Shogomori, H., and D. A. Brown. 2003. Use of detergents to study membrane rafts: The good, the bad, and the ugly. *Biol. Chem.* 384:1259–1263.

Simons, K., and W. L. C. Vaz. 2004. Model systems, lipid rafts, and cell membranes. *Annu. Rev. Biophys. Biomol. Struct.* 33:269–295.

Simopoulos, A. P., R. R. Kifer, and R. E. Martin. 1986. Health effects of polyunsaturated fatty acids in seafood. Academic Press, Orlando.

Stillwell, W. 2000. Docosahexaenoic acid and membrane lipid domains. *Curr. Org. Chem.* 4:1169–1183.

Stillwell, W., and S. R. Wassall. 2003. Docosahexaenoic acid: membrane properties of a unique fatty acid. *Chem. Phys. Lipids.* 126:1–27.

Stulnig, T. M., M. Berger, T. Sigmund, D. Raederstorff, H. Stockinger, and W. Waldhausl. 1998. Polyunsaturated fatty acids inhibit T cell signal transduction by modification of detergent-insoluble membrane domains. *J. Cell Biol.* 143:637–644.

Stulnig, T. M., J. Huber, N. Leitinger, E.-M. Imre, P. Angelisova, P. Nowotny, and W. Waldhausl. 2001. Polyunsaturated eicosapentaenoic acid displaces proteins from membrane rafts by altering raft lipid composition. *J. Biol. Chem.* 276:37335–37340.

Tokumasu, F., A. J. Jin, G. W. Feigenson, and J. A. Dvorak. 2003. Nanoscopic lipid domain dynamics revealed by atomic force microscopy. *Biophys. J.* 84:2609–2618.

Veatch, S. L., and S. L. Keller. 2003. A closer look at the canonical 'raft mixture' in model membrane studies. *Biophys. J.* 84:725–726.

Wassall, S. R., J. L. Thewalt, L. Wong, H. Gorrissen, and R. J. Cushley. 1986. Deuterium NMR study of the interaction of alpha-tocopherol with a phospholipid model membrane. *Biochemistry.* 25:319–326.

Webb, Y., L. Hermida-Matsumoto, and M. D. Resh. 2000. Inhibition of protein palmitoylation, raft localization, and T cell signaling by 2-bromopalmitate and polyunsaturated fatty acids. *J. Biol. Chem.* 275: 261–270.

Zerouga, M., L. J. Jenski, and W. Stillwell. 1995. Comparison of phosphatidylcholines containing one or two docosahexaenoic acyl chains on properties of phospholipid monolayers and bilayers. *Biochim. Biophys. Acta.* 1236:266–272.

Zerouga, M., W. Stillwell, J. Stone, A. Powner, and L. J. Jenski. 1996. Phospholipid class as a determinant in docosahexaenoic acid's effect on tumor cell viability. *Anticancer Res.* 16:2863–2868.

Zeyda, M., G. Staffler, V. Horejsi, W. Waldhausl, and T. M. Stulnig. 2002. LAT displacement from lipid rafts as a molecular mechanism for the inhibition of T cell signaling by polyunsaturated fatty acids. *J. Biol. Chem.* 277:28418–28423.